ADJUNCTIVE MEDICAL KNOWLEDGE

Principles of Nuclear Magnetic Resonance

Jason A. Koutcher and C. Tyler Burt

Dana Farber Cancer Institute, Massachusetts General Hospital, and Harvard Medical School, Boston, Massachusetts

The basic principles of nuclear magnetic resonance (NMR) are discussed. The concepts presented include a qualitative quantum-mechanical approach to NMR spectroscopy and a classical-mechanical approach to time-dependent NMR phenomena (relaxation effects). The spectroscopic concepts discussed include absorption of radiation by matter, spin and energy quantization, chemical shift, and spin-spin splitting. The time-dependent phenomena include the concepts of T_1 and T_2, the spin-lattice and spin-spin relaxation time, and Fourier-transform NMR spectroscopy.

J Nucl Med 25: 101–111, 1984

The rising number of biomedical applications of nuclear magnetic resonance (NMR) (*1–14*), particularly in the area of medical imaging, has brought this technique to the increasing attention of the medical community. This is the first in a series of four articles that will provide a basic explanation of the principles and medical applications of NMR. Special care will be taken in this paper to differentiate between explanations basically derived from quantum-mechanical concepts, and those that are based on classical concepts. In an initial exposure to NMR concepts, it is easy to become confused if one tries to understand classical models in terms of quantum-mechanical ideas, or vice versa. The discussion will require definition of various key words and phrases commonly used with NMR, such as chemical shift, spin state, and relaxation times; these will be explained in the text.

Received Oct. 7, 1983; revision accepted Oct. 7, 1983.

For reprints contact: Jason Koutcher, MD, PhD, NMR Office, Research 501, Massachusetts General Hospital, Boston, MA 02114.

Historically, NMR has developed into one of the most powerful analytic tools available to chemists over the recent two decades. Its primary use initially was in structure elucidation, although other applications have included determination of interatomic distances, measurement of reaction rates, and evaluation of the equilibrium constants of hydrogen bonding. As such, it has been an important aid in the synthesis of radionuclide-containing molecules.

NMR signals can provide both dynamic (time dependent) and equilibrium (time-independent) data. The time-independent aspects were first used in commercial instruments and gave rise to conventional NMR spectra (high-resolution NMR). One can also investigate the response of a collection of nuclei to a transient pulse of energy. Such behavior can be used to measure the relaxation times of the molecules in the sample (see below). It also serves as the conceptual basis for Fourier-transform NMR (discussed below).

The recent application of NMR to biochemical problems has been made possible by various technical advances that have increased the sensitivity of NMR

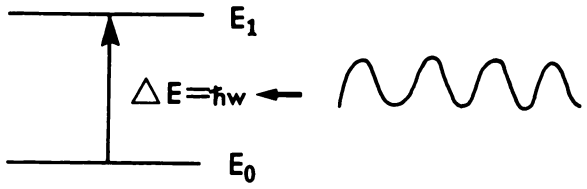

FIG. 1. Two-state system. Particle has two possible energy states (E_0 and E_1), and when exposed to correct energy ($\Delta E = E_1 - E_0 = \hbar\omega$), particle will be promoted to higher level.

significantly; it formerly required highly concentrated samples for study and was therefore used primarily for structure analysis. A recent paper by Glonek et al. (*15*) lists some of the many advances that have made NMR relevant to biochemistry. The sensitivity of NMR has been increased by several orders of magnitude through the use of Fourier-transform NMR spectroscopy, new electronic components such as minicomputers, pulse amplifiers, extended memories, etc., very-high-field superconducting magnets without appreciable field drift, and large-bore magnets with excellent homogeneity. These have made it possible to do in vivo physiologic and biochemical studies. The same advances—particularly the use of large-bore superconducting magnets—have also helped to extend the capability of NMR to the rapidly expanding field of NMR medical imaging over the past 6 years.

QUANTUM-MECHANICAL MODEL—HIGH-RESOLUTION NMR

It cannot be stated strongly enough that NMR is a phenomenon based on quantum mechanics. Fortunately, it is not necessary to understand quantum mechanics in all its complexity to derive both scientific and medical data from NMR spectra or images. It is convenient, however, to explain NMR spectra on a quantum-mechanical basis while treating relaxation (time dependent) phenomena in terms of classical mechanics.

A fundamental tenet of quantum mechanics (the study of atomic phenomena) is that particles exist in discrete energy states. These energy states are determined by mathematical principles and generally the energy states do not form a continuum as in classical mechanics but exist as discrete (quantized) states, separated by finite energy differences (Fig. 1). To change the state of a particle, absorption (or emission) of exactly the correct amount (quantum) of energy is required to cause a promotion (or drop) of the particle to another state.

The energy absorbed (or emitted) is in the form of electromagnetic (EM) radiation, like that in sunshine and radio waves. According to Planck's Law, the energy of EM radiation is proportional to its frequency, i.e.:

$$\Delta E = \hbar\omega, \qquad (1)$$

where ΔE is the energy, ω is the frequency of transition, and $\hbar$ (called "h bar") is Planck's constant (h) divided by 2π.

Equation (1) implies that the regions of the EM spectrum (radiofrequency, microwave, infrared, visible, ultraviolet, and x-ray) are of different energies because of their different frequency ranges (Fig. 2). The requirement of using EM energy at a precise frequency to cause a particle (electron, nucleus, atom, molecule) to be promoted to a higher state is the basis for all molecular *spectroscopy* across the EM range, including NMR.

NMR is based upon the concept that some atomic nuclei have an inherent angular momentum or "spin" and there is an energy associated with each spin state. In a manner analogous to energy existing in discrete or quantized states, spin angular momentum (I) is also quantized. For the sake of simplicity, we will consider only two spin states ($+1/2$ or $-1/2$), although more complex systems can be of biological relevance. In the absence of an external magnetic field, H_0, the energies of the two spin states will be identical (in spectroscopic terminology, they are said to be "degenerate"). However, in the presence of H_0, two distinct spin states with an energy separation exist (Fig. 3A). The presence of these two spin-energy states sets up a spectroscopic experiment similar to that described previously in Fig. 1. The energy

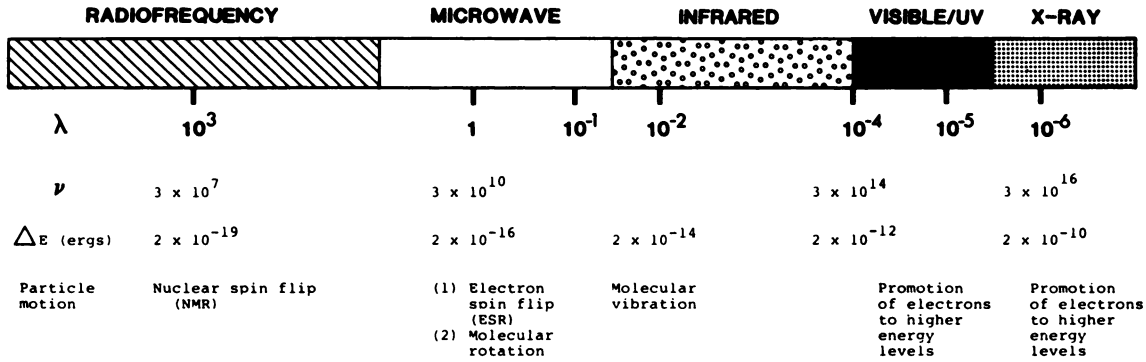

FIG. 2. Regions of EM radiation with their corresponding wavelengths (λ), frequencies ($\nu = \omega/2\pi$), energies (ΔE), and effect on appropriate "particle."

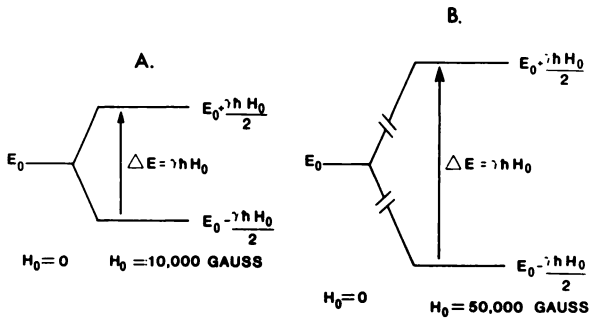

FIG. 3. Energy levels for hydrogen nucleus (proton) in absence of magnetic field ($H_0 = 0$), in field of 10,000 G (A), and in field of 50,000 G (B). (Energy spacing not drawn to scale.) E_0 is energy of nuclei in absence of magnetic field. Note that at higher field strength, energy separation is greater because $\Delta E \propto H_0$ [Eq. (2)], and leads to stronger NMR signal.

difference between the two spin states is given by:

$$\Delta E = \gamma\hbar H_0, \qquad (2)$$

where γ is called the magnetogyric moment, being unique for each nucleus.

There is no classical analogy to the concept of nuclear spin. Spin was initially postulated for an electron in order to explain the existence of two closely spaced lines instead of a single one in the spectra of alkali atoms. Some nuclei were later noted to have a similar property of spin angular momentum. This gives rise to a *magnetic moment* for electrons and nuclei with spin angular momentum, since a *spinning* charged particle must generate a magnetic field according to the basic laws of electromagnetism. The energy associated with this spin angular momentum is therefore sensitive to the presence of a magnetic field.

Combining Equations (1) and (2) yields:

$$\omega = \gamma H_0, \qquad (3)$$

where ω is the frequency of the EM energy required to cause a transition between the two different spin states. Equation (3) defines the resonance frequency at which the nuclei absorb energy. This equation defines a unique field-to-frequency ratio for each nucleus, which must be satisfied if one is to observe an NMR signal. Specifying either the resonant frequency or the strength of the external magnetic field (H_0) defines the other by Eq. (3). In either case, the net result is that the magnetic field (H_0) generates energy states that did not exist in the absence of the field.

The magnetic field H_0 is by convention aligned along the z axis of a three-dimensional coordinate system. The field must be very homogeneous, particularly for high-resolution NMR. Typical commercial magnets have field strengths that range from 1000 G (0.1 tesla) to greater than 84,000 G. This places ω, the resonance frequency, in the radiofrequency range (1-500 MHz), according to Eq. (3). Table 1 is a list of nuclei and their resonance frequencies at 21,100 G.

Not all nuclei give rise to an NMR signal. Both protons and neutrons have the property of spin—the proton and neutron spins within a nucleus can couple to give a net spin of 0 (^{12}C, ^{16}O), half integral [$^{1}H(1/2)$,

TABLE 1. NUCLEAR PROPERTIES OF SELECTED NUCLIDES

Nuclide	Resonance frequency at 2.1 T* (values in MHz)*	Nuclear spin I (in multiples of $\hbar/2$)	Natural abundance (%)	Relative sensitivity†
^{1}H	90.00	1/2	99.98	1.0
^{2}H	13.82	1	0.015	9.65×10^{-3}
^{13}C	22.63	1/2	1.11	1.59×10^{-2}
^{14}N	6.50	1	99.63	1.01×10^{-3}
^{15}N	9.12	1/2	0.37	1.04×10^{-3}
^{17}O	12.20	5/2	0.04	2.91×10^{-2}
^{19}F	84.57	1/2	100.00	0.83
^{23}Na	23.81	3/2	100.00	9.25×10^{-2}
^{25}Mg	5.51	5/2	10.05	2.68×10^{-3}
^{31}P	36.44	1/2	100.00	6.63×10^{-2}
^{33}S	6.90	3/2	0.74	2.26×10^{-3}
^{35}Cl	8.82	3/2	75.4	4.70×10^{-3}
^{37}Cl	7.34	3/2	24.6	2.71×10^{-3}
^{39}K	4.20	3/2	93.08	5.08×10^{-4}
^{43}Ca	6.06	7/2	0.13	6.40×10^{-2}

* T is the field strength in tesla (10,000 G = 1 Tesla).

† At constant field.

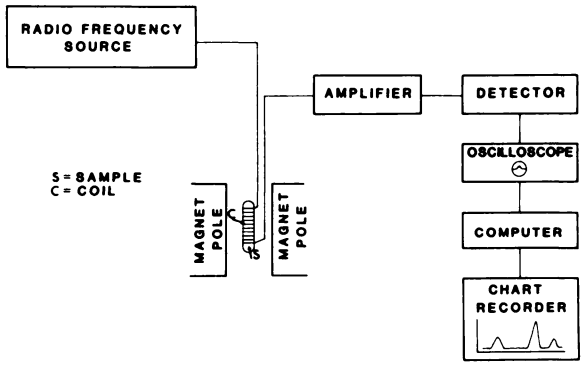

FIG. 4. Block diagram of NMR spectrometer. Sample is in middle of magnet, surrounded by coil that can both transmit energy from radiofrequency source (spectrometer) to sample and detect signal emitted by nuclei. Signal is then transmitted to detector, amplified, and displayed on oscilloscope. Signal can be processed for display on oscilloscope or printout on chart recorder.

$^{19}F(1/2)$, $^{31}P(1/2)$, $^{39}K(3/2)$], or integral [$^{2}H(1)$, $^{14}N(1)$]. Nuclei of net spin 1/2 are relatively simpler to analyze and have been studied extensively in the biomedical literature. Nuclei of spin >1/2 have more than two energy levels and their spectra are often more complex. Nuclei with net spin of zero (even atomic number and atomic mass) will not have a net spin angular momentum and will not give rise to an NMR signal.

The radiofrequency energy is supplied by a *small oscillating* magnetic field, H_1, oriented in the xy plane and, to satisfy Eq. (3), oscillating at the frequency of absorption (ω). H_1 is perpendicular to H_o, the main magnetic field. The presence of two magnetic fields, (H_o and H_1) is sometimes confusing initially, but the characteristics of the fields are completely different. The main (static) magnetic field, H_o, is in the z direction and polarizes the nuclei into two different energy states; the small oscillating field, H_1, is provided by a coil that fits around the sample, both being located in the main magnetic field. H_1 is in the xy plane and serves as a source of electromagnetic radiation to induce a transition between the two states.

The two principal components of an NMR experiment include the magnet (H_o) and the spectrometer, which essentially is a very sophisticated radio transmitter and receiver. A block diagram of an NMR system is shown in Fig. 4. Notice that the coil generating the H_1 field surrounds the sample.

Two schemes suggest themselves to measure NMR signals. Equation (3) states that the magnetic field and frequency are interchangeable NMR parameters. It is therefore possible either to sweep the frequency range and keep the field constant in a manner analogous to infrared or ultraviolet spectrometry, or to sweep the magnetic field and keep the frequency constant, searching for resonance. The two techniques are equivalent and are called continuous wave (CW) NMR spectroscopy. An alternative to the above methods, called Fourier-transform NMR, will be discussed later.

Sensitivity. The sensitivity of an NMR experiment depends on several parameters, including coil design, magnetic field, nucleus sensitivity, and sample size. It is determined fundamentally, however, by the distribution of nuclei between the two spin states. The greater the difference in population between the two states, the stronger the signal. Since this difference in population is small (see Table 2), NMR is intrinsically a very insensitive technique.

The distribution of nuclei between the two spin states is determined by the Boltzmann distribution:

$$\frac{n_{upper}}{n_{lower}} \propto e^{-\Delta E/kt} = e^{-\gamma\hbar H_o/kT}, \qquad (4)$$

where n_{upper} and n_{lower} are the numbers of nuclei in the

TABLE 2. NUCLEAR DISTRIBUTION AT VARIOUS FREQUENCIES

Resonance frequency	Relative excess $\Delta N/N^*$	Sample distribution based on 20×10^7 nuclei	
1 MHz	0.8×10^{-7}	upper	99,999,992
		lower	100,000,008
6 MHz	5.6×10^{-7}	upper	99,999,944
		lower	100,000,056
20 MHz	16.0×10^{-7}	upper	99,999,840
		lower	100,000,160
100 MHz	80.1×10^{-7}	upper	99,999,199
		lower	100,001,801
400 MHz	320.3×10^{-7}	upper	99,996,797
		lower	100,003,203

* Relative excess is calculated by the equation $\Delta N/N = \Delta E/2kT$, where N is the total number of nuclei and ΔN is the difference between upper and lower energy-state populations.

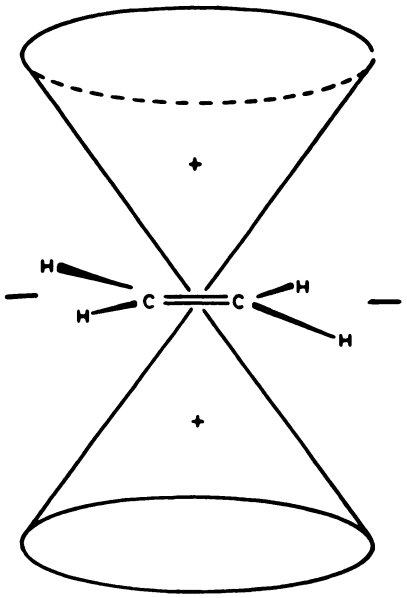

FIG. 5. Shielding effects in carbon-carbon double bond. Positive (+) sign indicates more screening, while negative (−) sign indicates deshielding. Shielding effect decreases with distance. (Reprinted by permission from Ref. 16.)

upper and lower spin states, k is the Boltzmann constant, and T is the absolute temperature. Equation (4) dictates that the relative populations of the two spin states are dependent in an exponential manner on the *energy difference* between the two states. Since the energy difference (ΔE) is proportional to H_0 [see Eq. (2)], an increase in the magnetic field strength will result in a larger energy separation between the two spin states, and an increased asymmetry in the population of the spin states [Fig. 3b and Eq. (4)], which will give rise to a stronger NMR signal. The advent of superconducting magnetic coils has made it feasible to obtain fields of greater than 85 kG, and this has been critically important to the application of NMR to biochemistry. Table 2 demonstrates the small difference in energy levels between upper and lower population levels.

Chemical shifts. Equation (3) predicts that all nuclei of a given nuclide would resonate at precisely the same H_0 for a given frequency. Actually resonance occurs at slightly different values of H_0 for a given nucleus depending on its electron and molecular environment. These slight differences in absorption frequencies or *chemical shifts* are what make NMR a valuable analytic tool.

Chemical shifts arise because a nucleus is surrounded by an electron cloud. The charge distribution in this cloud, and even electrons from neighboring atoms, can influence the magnetic field "felt" by the nucleus, by generating small *local* magnetic fields, with radii in the angstrom range, that can add or subtract from the applied field, H_0 (Fig. 5). The actual magnetic field at the nucleus can therefore be higher or lower than H_0.

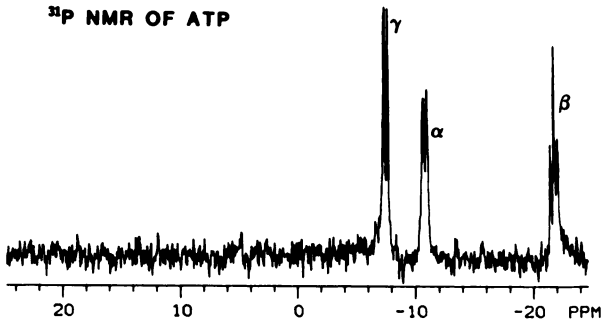

FIG. 6. P-31 NMR spectrum of ATP at pH 6.7 and 50 m*M* concentration. Chemical shifts are measured relative to 85% H_3PO_4. Peaks represent α, β, and γ phosphorus atoms of ATP. Spectrometer frequency 60.72 MHz.

The effective magnetic field at the nucleus, H_{local}, can be written as:

$$H_{local} = H_o + H_e, \qquad (5)$$

where H_{local} is the magnetic field at the nucleus (i.e., the effective magnetic field) and H_e represents the field induced by the local environment. H_e may have several subcomponents due to diamagnetic or paramagnetic effects, or to shielding caused by aromatic ring currents or dipolar groups in the molecule. An intensive discussion of these various types of shielding effects is beyond the scope of this paper (*16,17*). These shielding effects can be either positive (shielding) or negative (deshielding), thereby either decreasing or increasing the effective field at the nucleus, leading to slight differences in the resonance frequencies called chemical shift. These chemical shifts are the basis of high-resolution NMR both in vitro and in vivo.

Figure 6 is a spectrum of ATP, which contains three phosphorus atoms in slightly differing chemical environments. Each phosphorus atom resonates at a characteristic frequency slightly displaced from the others because of its different atomic environment.

Chemical shifts are usually measured relative to the peak position of an arbitrary reference compound. Tetramethylsilane (TMS) is conventionally used as a reference standard for proton- and carbon-NMR. Chemical shifts are measured as the distance between the observed peak position and TMS. For P-31 NMR, 85% H_3PO_4 is often used as a reference standard.

As described, chemical shifts would be measured in units of frequency, i.e., hertz (cycles/sec) and would be field-dependent, i.e., doubling the magnetic field (H_0) would double the distance between the two peaks. It is now preferable to refer to the chemical shift as δ and to define it as the distance between the peak and the reference compound divided by the spectrometer frequency (or magnetic field H_0 if the distance is measured in milligauss).

This can be expressed mathematically as:

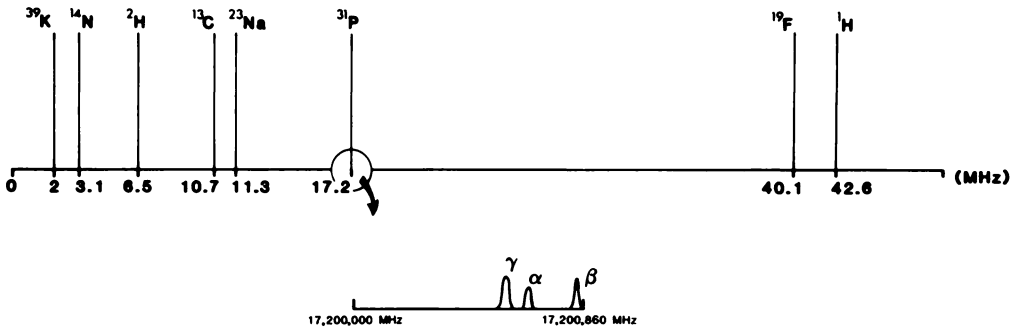

FIG. 7. Resonance frequencies of different nuclei in 10,000-G (H_o) field. Resonant frequencies are widely separated compared with spectral width of given nucleus, as depicted by lower half of diagram, which shows P-31 NMR spectrum of ATP (Fig. 6). Wide separation between resonant frequencies for different nuclei allows them to be studied independently without interference.

$$\delta = \frac{H_i - H_r}{H_o} \times 10^6 = \frac{\omega_i - \omega_r}{\omega_o} \times 10^6, \qquad (6)$$

where ω_i and H_i are the frequency and field at which resonance occurs for the peak being described, ω_r and H_r are the frequency and field of the reference peak, and H_o and ω_o are the field and frequency of the spectrometer. δ is dimensionless and is measured in parts per million (ppm). The ppm unit arises because the resonance frequency is in megahertz while the difference between the standard and compound may be only a few hertz. The ratio is therefore of the order of 10^{-6}. Multiplication by 10^6 makes δ a more convenient number (between 0 and several hundred, depending on the nucleus). The great significance of δ is that chemical shifts measured in ppm are field-independent because the denominator of Eq. (5) corrects for the field-dependence.

Observation of different nuclei. Equation 3 also predicts that one can "tune" to a particular nucleus, since γ for each nucleus is different. At a constant H_o, changing ω to an appropriate frequency will "tune" to another nucleus. This is illustrated in Fig. 7, which shows that at a given H_o, the resonant frequencies of different nuclei are separated well enough so that there will be no interfering signal from other nuclei. The chemical-shift considerations mentioned above still enter in. Figures 8 and 9 are H-1 and C-13 NMR spectra from acidified CH_3CH_2OH, demonstrating the ability of NMR to study compounds by obtaining signal independently from different nuclei within a molecule. This can be used to study various parts of molecules independently, such as protein-ligand binding (*18–21*).

Spin-spin splitting. A particularly interesting example of how quantum mechanics can lead to unexpected results is shown by the so-called spin-spin splitting phenomenon. We include this to show how subtle quantum NMR phenomena can be and because the effects have been mentioned in the biological literature and may eventually be of some clinical relevance.

Under low resolution, the ^{1}H-NMR spectrum of acidified ethanol consists of three peaks with area ratios of 1:2:3, corresponding to the OH, CH_2, and CH_3 protons. Under higher resolution (Fig. 8), the methylene and methyl proton peaks appear as a quartet and a triplet, respectively, whose relative total area remains in the ratio

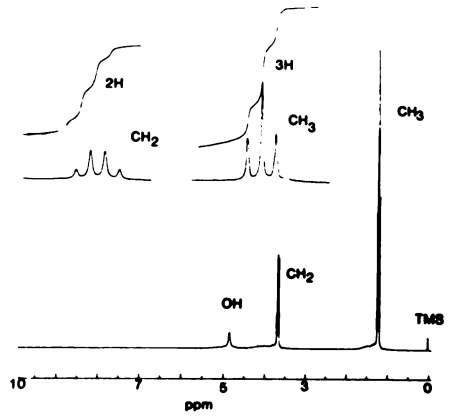

FIG. 8. High-resolution ^{1}H (proton) spectrum of acidified ethanol (CH_3CH_2OH). Insert shows CH_3 and CH_2 peaks on expanded scale, demonstrating spin-spin splitting. Integrated intensities show that areas of CH_3 and CH_2 resonances have 3:2 ratio, as expected from relative numbers of protons. TMS (tetramethylsilane) is reference compound added to sample from which chemical shifts are measured. Under acidified conditions, OH proton does not interact with other protons on molecule. Courtesy of Bruker Instruments.

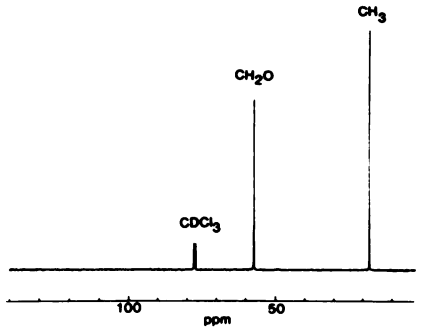

FIG. 9. High-resolution C-13 NMR spectrum of ethanol (CH_3CH_2OH) dissolved in deuterated chloroform ($CDCl_3$) demonstrating two absorption peaks due to different electronic environments of two carbon atoms. Courtesy of Bruker Instruments.

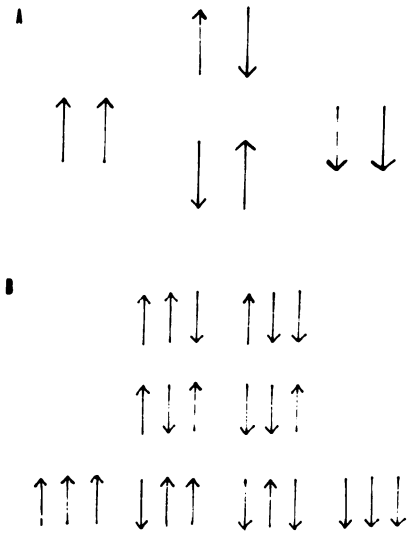

FIG. 10. (a) Possible spin combinations for protons of CH_2 group. Note that middle state is twice as likely to occur, since there are two possible spin combinations that give rise to it. Adjacent CH_3 resonance will therefore be split into three peaks with area intensities 1:2:1. (b) Possible spin combinations for CH_3 group. Adjacent CH_2 resonance will therefore be split into four peaks with area ratios 1:3:3:1.

of 2:3. The splitting is found to be independent of field strength, as opposed to the chemical shifts, which were noted above to be field-dependent.

The observation of these splitting patterns is explained by assuming that the magnetic field at the nucleus is influenced by the spin arrangements of the protons in adjacent groups. For the two protons of the methylene group of ethanol, there are three possible combinations of spin orientation (Fig. 10A). These combinations split the adjacent methyl proton peak into three peaks, with area ratios of 1:2:1 due to the three possible spin combinations for the methylene protons seen in Fig. 10B. Similarly, the methylene resonance is split into four peaks by the four spin arrangements possible for the protons on the neighboring methyl group (Fig. 10B), with the relative intensities of the four methylene peaks in the ratio of 1:3:3:1. The two middle peaks will be three times the intensity of the end peaks becasue there are three times as many spin combinations that give rise to these states.

In general, if a resonance peak undergoes spin-spin splitting due to n identical neighboring nuclei, the peak will be split into $2nI + 1$ peaks. For nuclei of spin $I = 1/2$, the peak intensities are proportional to the coefficients of the binomial expansion. For P-31 the usual coupling is to other phosphorus nuclei or to protons.

At present, the imaging techniques available are not sufficiently sophisticated or sensitive to detect many of these quantum-mechanical effects. However, some of these effects are seen in biological samples by some of the methods used in high-resolution NMR spectroscopy (*22*).

CLASSICAL MODEL-PULSE NMR

The previous discussion developed a theoretical framework for NMR based upon quantum-mechanical concept of energy. In this section, the NMR experiment will be considered in a time-dependent manner to study how the collection of nuclei behave when exposed to external influences, i.e., radiofrequency radiation. The theory of classical mechanics can accurately represent the concepts necessary to develop this alternative framework for NMR.

We have already referred to the nuclear spin, noting that each nucleus in a magnetic field has a small quantized magnetic moment, which is usually designated μ. The net magnetic moment of the sample (M) represents the sum of the individual magnetic moments, averaged in terms of whether they are aligned with or against the magnetic field, i.e., a vector sum. This vector can be treated as a classical physical parameter for which little or no knowledge of quantum mechanics is required.

A model that will be helpful in thinking about macroscopic magnetic moments is that of a rotating top, which also has angular momentum. In this analogy, the rate of precession (the rate at which the top's axis revolves when disturbed from its equilibrium position) is related to the energy of transition of the nuclei. Again, we will consider only one transition (i.e., only two spin states) so there is only one frequency of precession. This is called the *Larmor frequency*, and its functional form bears a resemblance to Eq. (3). This is because both frequencies are related to energies that are dependent on the angular momentum of the physical entity (atomic nucleus or top).

One can consider that a top in a gravitational field is analogous to the nuclei arranged in a magnetic field. The top can be tipped to any angle in the gravitational field, although at the atomic level the nuclei are permitted only two positions. It is the averaging process that allows a large number of nuclei to behave like a top. Thus, one can imagine a large sample, a centimeter on each side, made up of many small boxes, each a micron on a side, with a small top in each little box (see Fig. 11). The large box will then act as the average of all the boxes and will have a net moment that depends on the vector sum of all the little moments of the individual tops. This is similar to the concept of the net magnetization of the sample M being the vector sum of the individual magnetic moments. The vector M is aligned spatially along the same axis as H_o, i.e., the z axis (Fig. 12, $t = 0$), with no component in the xy plane.

In a similar manner to the previously discussed CW experiment, one can ask what would happen if one applied a pulse of radiofrequency power to the nuclear sample. EM radiation is associated with both an electrical and magnetic field, and would therefore exert a torque on M, tipping the magnetic moment from the z axis, and bringing a component of the vector into the xy

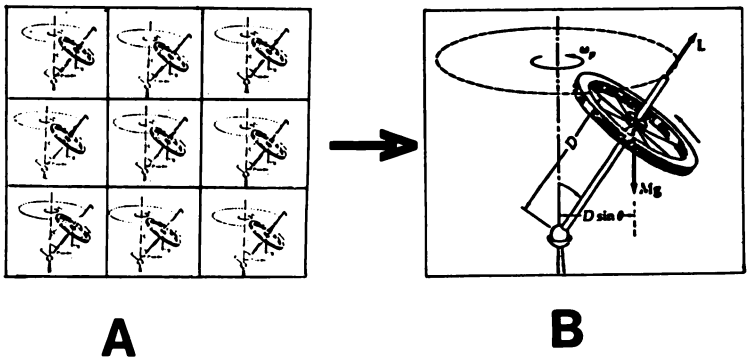

FIG. 11. Part (A) shows collection of small tops, each spinning independently in gravitational field. Net angular momentum of whole box can be imagined as one large top spinning in entire box (B). Large top is actually statistical average of small boxes so that suddenly switching gravitational field by turning box upside down would lead to eventual realignment of net angular momentum to new direction. How fast this occurs depends, as mentioned in text, on how fast each top in its own individual box reorients.

plane (M_{xy}) (Fig. 12, t = a). The longer the pulse is turned on, the greater the angle (α) the magnetic vector will turn through. Thus, for example, applying a 10-μsec pulse might cause a tilt of 45°, 20 μsec a tilt of 90°, 40 μsec a 180° tilt, etc. This is the basis of the 90° and 180° pulse commonly mentioned in NMR texts. The NMR signal can be detected only when the magnetization has a component in the xy plane. The signal is greatest for a flip angle of 90° (because M will then lie completely in the xy plane), and total loss of signal occurs for a flip angle of 180°, since then there is no component in the xy plane.

After the RF pulse is turned off, a component of the magnetization vector (M) will remain in the xy plane for a finite time (Fig. 12, t = b, c, d) and will decay, returning to its initial orientation along the z axis (Fig. 12, t = 0) at a rate determined by the relaxation times T_1 and T_2. The NMR signal will vanish when the magnetization vector decays completely in the xy plane. This resonance signal, with its exponential decay (Fig. 13), is called a free induction decay or FID.

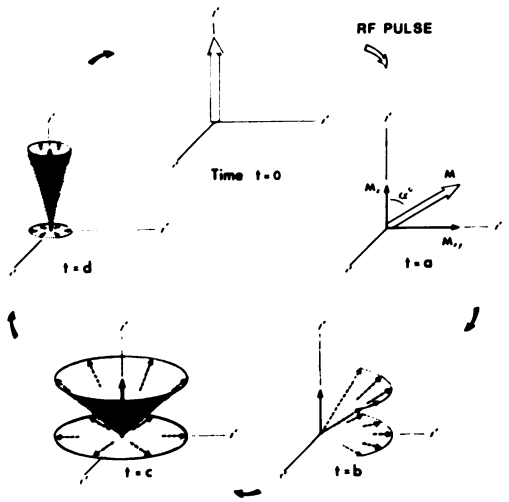

FIG. 12. (t = 0) In presence of static magnetic field, H_0, nuclei with their magnetic moments (μ) generate magnetization vector, M, in direction of H_0. (t = a) Sample is exposed to rotating magnetic field, H_1, tipping magnetization vector into xy plane and giving rise to NMR signal (see Fig. 13—point b). (t = b, c, d) H_1 field is turned off, and nuclei undergo spin-lattice (T_1) and spin-spin (T_2) relaxation, leading to loss of magnetization in xy plane and decreased NMR signal (Fig. 13, point c). Spin-spin relaxation is depicted by fanning out of M_{xy} vector in xy plane because of slight differences in various spin energies secondary to spin-spin energy exchange. T_1 relaxation (loss of energy to environment) occurs simultaneously and is shown by increase in magnetization in z direction. (Reprinted from Ref. 12, by permission.)

In this type of pulse experiment, the radiofrequency transmitter is "on" for a very short time, delivering a brief but very intense burst of RF energy to the sample. The decay characteristics or relaxation time constants of the sample can be calculated by modifications of this basic pulse experiment (see below). The reader is referred to various texts for further experimental details (*23–25*).

In a relaxation experiment, the usual quantities measured are T_1 and T_2, the spin-lattice and spin-spin relaxation times. T_1 is a measure of how rapidly the sample can release the radiofrequency energy it absorbed to the surrounding environment and thereby allow the nuclei in the sample to relax to their initial undisturbed lower-energy distribution. It is analogous to an object being heated rapidly (radiofrequency energy in), the heat source being removed and the time it takes to cool (loss of energy) to its initial temperature (analogous to the initial spin state) measured. Ninety-nine per cent of the absorbed energy will be released to the surrounding environment after a period 5 × T_1.

Alternatively, T_1 can be thought of as relaxation in the longitudinal (z) direction whereas T_2 is the transverse relaxation time (xy plane). Once a pulse has been delivered, both transverse and longitudinal relaxations begin simultaneously.

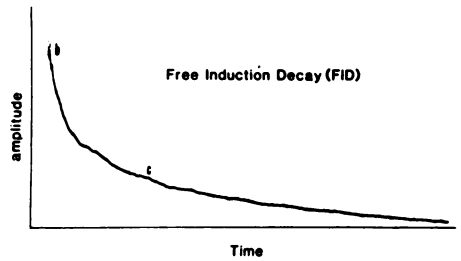

FIG. 13. On-resonance free induction decay (FID) of benzene. Point of maximum signal strength (b) corresponds to Fig. 12, t = a. Signal subsequently decays as nuclei relax corresponding to Fig. 12, t = b, c, d.

As mentioned previously, T_1 processes relate to loss of energy to the environment (i.e., all the surrounding atoms not being observed in the NMR experiment). This causes the magnetization vector (M) to increase in the z direction till it reaches its initial value. Concurrently there is exchange of energy between the individual nuclei (spin-spin or T_2 processes). Returning to the previous model of the ensemble of tops, it is similar to an exchange of small quantities of energy between the tops. The slight energy differences caused by these energy transfers would cause the tops to precess at slightly different rates. If they had all started precessing simultaneously, they would fall out of phase with each other.

At a nuclear level, the individual spins would also no longer precess at the same rate. The radiofrequency energy emitted by the various nuclei would also be out of phase and would not add coherently, leading to loss of signal. The latter process occurs at a rate different from the buildup of magnetization in the z direction (T_1 process), which is effected only by release of energy to neighboring atoms (environment) and not by energy exchange within the sample (Fig. 12).

T_1 and T_2 are usually not equal. In tissue, T_1 is usually about 10 times as great as T_2. T_2 must always be less than or equal to T_1, since when the magnetization has returned to its initial equilibrium position (in the z direction) there can be no residual component in the xy plane. The time-dependent behavior of the magnetization is described by the Bloch equations:

$$\frac{dM_x}{dt} = \gamma(M_yH_o + M_zH_1 \sin\omega t) - \frac{M_x}{T_2},$$

$$\frac{dM_y}{dt} = \gamma(M_zH_1 \cos\omega t - M_xH_o) - \frac{M_y}{T_2}, \qquad (7)$$

$$\frac{dM_z}{dt} = \gamma(-M_xH_1 \sin\omega t - M_yH_1 \cos\omega t) \frac{M_z - M_o}{T_1},$$

where ω_o is the resonance frequency, M_x, M_y, and M_z are each the magnetization in the x, y, and z direction, and M_o is the initial magnetization.

In addition there is always some inhomogeneity in the magnetic field. Returning to the previous model, this means each little box is at a slightly different resonance frequency, so that the tops will slowly fall out of phase with each other. Similarly, the nuclei will resonate at slightly different frequencies due to field inhomogeneities, and will fall out of phase with each other. Thus, even though there may be magnetization in the xy plane, there will be no signal because of destructive interference, so that T_2 as determined by the decay of an FID will be less than the intrinsic T_2. It is often designated T^*_2.

Fourier-transform NMR. A serious drawback to CW NMR spectroscopy is the time wasted while one is scanning between peaks. This is not a serious problem with strong signals but in a sample where the resonance peak is weak and requires signal averaging (i.e., recording the spectra numerous times and averaging them to improve the quality of the spectrum) this can be a serious drawback.

In an ideal system, one could excite all frequencies simultaneously to minimize time spent not recording actual data. This can be achieved by using pulse NMR. The signal recorded is the FID discussed previously. All resonances surrounding a central frequency are detected. An equivalent high-resolution spectrum similar to that obtained by conventional (continuous wave) techniques can be generated from the Fourier analysis of FID. The latter calculation is complex and is done on a computer.

The excitation of all frequencies simultaneously (in addition to the spectrometer frequency) is caused by the fact that switching the radiofrequency pulse on and off introduces sidebands of the main frequency; these contain all the neighboring frequencies and can therefore excite all neighboring resonances simultaneously.

The concept of Fourier-transform NMR spectroscopy can be thought of by the analogy of determining the frequencies of several tuning forks. One could match them individually to the correct frequency using a variable frequency note (similar to a CW experiment). Al-

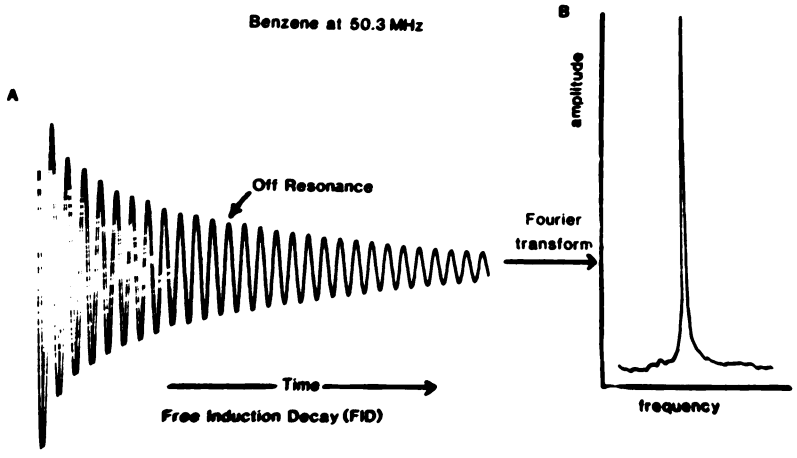

FIG. 14. (a) Off-resonance FID of benzene (C-13) showing decaying sine wave of single frequency. (b) Frequency-domain C-13 NMR spectrum of benzene, consisting of single peak corresponding to single frequency seen in part (a).

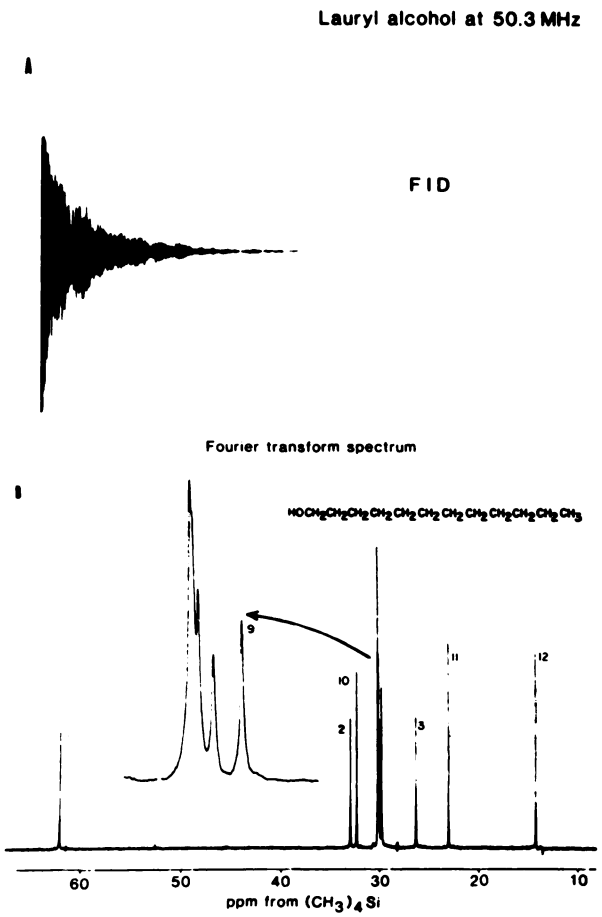

FIG. 15. (A) Complex C-13 NMR FID arising from neat lauryl alcohol at 35°C. (B) Fourier transform of Fig. 15(A) showing C-13 high-resolution spectrum of neat lauryl alcohol.

ternatively, one can excite all of the tuning forks simultaneously causing them to oscillate concurrently. One could analyze the resultant waveform called a time spectrum (viewed on an oscilloscope) that is analogous to an FID, and resolve the various frequencies of the tuning forks electronically (frequency spectra) in a manner similar to the Fourier-transform process.

Figure 14 is an off-resonance C-13 NMR FID of benzene (in which all the carbon atoms are equivalent). If one ignores the decay, the FID is similar to a sine wave with a single frequency. The decay in the sine wave is caused by relaxation processes. The damped sine wave is a plot of signal intensity against time or a time-domain spectrum. Since there is only one frequency present, it can be determined by measuring the interval between cycles of the sine wave. Figure 14B is the frequency equivalent of Fig. 14A, showing a one-frequency absorption spectrum.

While simple spectra and FIDs can be interconverted visually, a complex FID such as is generated by a C-13 NMR spectrum of neat liquid lauryl alcohol (Fig. 15) is far too difficult. However, by use of the Fourier-transform method, with a computer to do the calculation, the frequency-domain spectra can be calculated.

An important advantage of pulsed experiments is that the calculation of relaxation times is markedly simplified. This is done by tailoring the pulse sequences, as will be discussed more fully in a later paper.

Summary. Our discussion has shown how an effect at the nuclear level can be transformed into spectra that potentially yield chemical, biological, and medical information. This is possible because magnetic fields can turn many useful nuclei into "transmitters" that can be identified and located within a molecule spectroscopically.

In addition, the time-dependent behavior of the nuclei allows one to compute relaxation times. This is the amount of time it takes for a perturbed system of nuclei to return to its initial state. The relaxation times are a measure of the relative mobilities of molecular species and are very sensitive to changes in the molecular environment, such as solvent effects, ionic strength, and the presence of various ions. We shall see in future sections how valuable this is for NMR imaging.

ACKNOWLEDGMENTS

This work supported in part by Technicare Corporation, Solon, Ohio.

The authors gratefully acknowledge the secretarial and administrative assistance of Edith Bell and DeeDee Correia, and the critical suggestions of Dr. Thomas J. Brady. Dr. James Hamilton of Boston University generously contributed Figures 13-15.

REFERENCES

1. MOON RB, RICHARDS JH: Determination of intracellular pH by ^{31}P magnetic resonance. *J Biol Chem* 248:7276-7278, 1973
2. HOULT DI, BUSBY SJW, GADIAN DG, et al: Observation of tissue metabolites using ^{31}P nuclear magnetic resonance. *Nature* 252:285-287, 1974
3. BARANY M, BARANY K, BURT CT, et al: Structural changes in myosin during contraction and the state of ATP in the intact frog muscles. *J Supramol Struct* 3:125-140, 1975
4. NAVON G, OGAWA S, SHULMAN RG, et al: High resolution ^{31}P nuclear magnetic resonance studies of metabolism in aerobic *Escherichia coli* cells. *Proc Natl Acad Sci USA* 74:888-891, 1977
5. BURT CT, COHEN SM, BARANY M: Analysis with intact tissue with ^{31}P NMR. *Annual Rev of Biophys and Bioengineering* 8:1-25, 1979
6. BURT CT: NMR studies of muscle constituents in living tissue. In *Cell and Muscle Motility*. Vol. 1. Dowben RW, Shay JW, eds. New York, Plenum Publishing Co., 1981, pp 375-389
7. BURT CT: NMR of live systems. *Life Sciences* 31:2793-2808, 1983
8. DAMADIAN R: Tumor detection by nuclear magnetic resonance. *Science* 171:1151-1153, 1971
9. KOUTCHER JA, GOLDSMITH M, DAMADIAN R: NMR in cancer: X. A malignancy index to discriminate normal and cancerous tissue. *Cancer* 41:174-182, 1978
10. LAUTERBUR PC, KRAMER DM, HOUSE WV, et al: Zeugmatographic high resolution nuclear magnetic resonance

spectroscopy. Images of chemical inhomogeneity within macroscopic objects. *J Am Chem Soc* 97:6866-6868, 1975

11. HINSHAW WS, BOTTOMLEY PA, HOLLAND GN: Radiographic thin section image of the human wrist by nuclear magnetic resonance. *Nature* 270:722-723, 1977
12. PYKETT IL, BUONANNO FS, BRADY TJ, et al: Techniques and approaches to proton NMR imaging of the head. *Computerized Radiology* 7:1-17, 1983
13. PYKETT IL, NEWHOUSE JH, BUONANNO FS, et al: Principles of nuclear magnetic resonance. *Radiology* 143:157-168, 1982
14. PYKETT IL: NMR imaging in medicine. *Sci Am* 246(5): 78-88, 1982
15. GLONEK T, BURT CT, BARANY M: NMR analysis of intact tissue including examples of normal and diseased human muscle determinations in NMR—basic principles and progress, Vol. 19. In *NMR in Medicine.* Damadian R, ed. Heidelberg, Springer-Verlag, 1981, pp 121-159
16. AKITT JW: *NMR and Chemistry.* London, Chapman and Hall, 1972, pp 17-28.
17. POPLE JA, SCHNEIDER WG, BERNSTEIN HJ: High resolution nuclear magnetic resonance. New York, McGraw-Hill, 1959, pp 165-180.
18. COLEMAN JE, ANDERSON RA, RATCLIFFE RG, et al: Structure of gene 5 protein-oligodeoxynucleotide complexes as determined by ^{1}H, ^{19}F, and ^{31}P nuclear magnetic resonance. *Biochemistry* 15:5419-5430, 1976
19. FELDMAN K, HELMREICH EJM: The pyridoxal 5'-phosphate site in rabbit skeletal muscle glycogen phosphoryase. b: An ultraviolet and ^{1}H and ^{31}P nuclear magnetic resonance spectroscopic study. *Biochemistry* 15:2394-2401, 1976
20. CHLEBOWSKI JF, ARMITAGE IA, COLEMAN J: Allosteric interactions between metal ion and phosphate at the active sites of alkaline phosphatase as determined by ^{31}P NMR and ^{113}Cd NMR. *J Biol Chem* 252:7053-7061, 1977
21. GETTINS P, POTTER M, RUDIKOFF S, et al: Investigation of haptenantibody interactions in McPC603 by ^{1}H and ^{31}P NMR spectroscopy. *FEBS Letts* 84:87-91, 1977
22. COHEN SM, OGAWA S, SHULMAN RL: ^{13}C NMR studies of gluconeogenesis in rat liver cells: Utilization of labeled glycerol by cells from euthyroid and hyperthyroid rats. *Proc Natl Acad Sci USA* 76:1603-1607, 1979
23. FARRAR TC, BECKER ED: *Pulse and Fourier Transform NMR.* New York, Academic Press, 1971
24. ABRAGAM A: *The Principles of Nuclear Magnetism.* New York, Oxford University Press, 1961
25. SLICHTER CP: *Principles of Magnetic Resonance.* Berlin, Springer, 1980